We are IntechOpen, the world's leading publisher of Open Access books
Built by scientists, for scientists

6,900
Open access books available

186,000
International authors and editors

200M
Downloads

Our authors are among the

154
Countries delivered to

TOP 1%
most cited scientists

12.2%
Contributors from top 500 universities

CLARIVATE ANALYTICS
BOOK CITATION INDEX
INDEXED

WEB OF SCIENCE™

Selection of our books indexed in the Book Citation Index
in Web of Science™ Core Collection (BKCI)

Interested in publishing with us?
Contact book.department@intechopen.com

Numbers displayed above are based on latest data collected.
For more information visit www.intechopen.com

Interference Modeling for Wireless Ad Hoc Networks

Altenis V. Lima-e-Lima*, Carlos E. B. Cruz Pimentel*
and Renato M. de Moraes**
*University of Pernambuco (UPE), Recife, Brazil
**University of Brasília (UnB), Brasília, Brazil

1. Introduction

Interference effects constrain scalability performance of ad hoc networks as Gupta and Kumar (Gupta & Kumar, 2000) showed that the throughput capacity of a fixed wireless network decreases when the number of total nodes n increases. More specifically, they showed that the node throughput decreases approximately like $1/\sqrt{n}$. Grossglauser and Tse (Grossglauser & Tse, 2001) presented a two-phase packet forwarding technique for mobile ad hoc networks (MANETs), utilizing *multiuser diversity* (Knopp & Humblet, 1995), in which a source node transmits a packet to the nearest neighbor, and that relay delivers the packet to the destination when this destination becomes the closest neighbor of the relay. The scheme was shown (Grossglauser & Tse, 2001) to increase the throughput capacity of MANETs, such that it remains constant as the number of users in the network increases, taking advantage that communication among nearest nodes copes the interference due to farther nodes.

On the other hand, detailed and straightforward models for interference computation in dense ad hoc networks have not been extensively studied. Grid models have been proposed to compute interference (Gobriel et al., 2004), (Liu & Haenggi, 2005), which take advantage of the regular placement of the nodes. This orderly topology is a good starting point for static networks; however, it does not apply for MANETs. Also, some previous works have assumed a transmission or a reception range for communication among nodes without considering the effect from the entire network (Tobagi & Kleinrock, 1975), (Deng et al., 2004). This approximation can be good for low density networks, but it may imply in inaccurate results for dense networks. One problem with such approximation is the difficulty in finding an analytical description for the random topology inherent to ad hoc networks. In other cases, analytical models use graph theory (Rickenbach et al., 2005), (Qin-yun et al. 2005). While they are good for higher layer analysis, like routing, such models may not be appropriate for a more detailed communication channel study because they do not consider physical parameters like Euclidean distance, fading and path loss, for example.

This chapter analyzes an improved channel communication model, from the model proposed by Moraes et al. (Moraes et al., 2008) that permits to obtain the measured signal to noise and interference ratio (SNIR) by a receiver node, and consequently its spectral Shannon capacity (or spectral efficiency) (Cover & Thomas, 1991) at any point in the network when it communicates with a close neighbor. This model considers Euclidean distance, path loss and Rayleigh fading. The nodes are assumed to move according to a random mobility pattern and the parameter θ represents the fraction of sender nodes in the network. Monte-Carlo simulations (Robert & Casella, 2004) are used to validate the model. Furthermore, previous works had assumed the receiver node located at the center of the network (Lau & Leung, 1992), (Shepard, 1996), (Hajek et al., 1997). The results presented here are more general which shows that the received SNIR and spectral efficiency tend to a constant as n increases if a node communicates with its close neighbors when the path loss parameter α is greater than two, regardless of the position of the node in the network, i.e., wherever the receiver node is at the center, or at the middle, or at the boundary of the network area. For the case where α equals two, the limit SNIR and spectral efficiency go to zero; however, they decay very slowly making local communication still possible for a finite n. Another study performed here presents an autonomous technique for node state determination (sender or receiver) for each node in the network as function of the θ parameter.

The remaining of this chapter is organized as follows. Section 2 introduces the network model. Section 3 presents the average number of feasible receiving neighbor nodes as a function of the network parameters. Section 4 explains the interference and spectral efficiency computation. Section 5 shows the results. Section 6 explains the autonomous technique for node state determination. Finally, Section 7 concludes the chapter summarizing the main results obtained.

2. Model

The modeling problem addressed here is that of a wireless ad hoc network with nodes assumed mobile. The model consists of a normalized unit circular area (or disk) containing n nodes, and resembles the Grossglauser and Tse's model (Grossglauser & Tse, 2001). Therefore, information flow in the network follows the two-phase packet relaying technique as described in (Grossglauser & Tse, 2001). The position of node i at time t is indicated by $X_i(t)$. Nodes are assumed to move according to the *uniform mobility model* (Bansal & Liu, 2003). This model satisfies the following properties (Bansal & Liu, 2003): (a) the position of the nodes are independent of each other at any time t; (b) the steady-state distribution of the mobile nodes is uniform; (c) the direction of the node movement is uniformly distributed in $[0,2\pi)$, conditional on the position of the node.

Any node can operate either as a sender or as a receiver. At a given time t, a fraction of the total number of nodes n in the network, n_s, is randomly chosen by the scheduler as senders, while the remaining nodes, n_r, operate as possible receiving nodes (Grossglauser & Tse, 2001). A sender density parameter θ is defined as $n_s = \theta n$, where $\theta \in (0, 1)$, and $n_r = (1 - \theta)n$. Section 6 describes a technique that allows the nodes to adjust their communication status (sender or receiver) in order to the network attain $n_s = \theta n$.

A node j at time t is capable of receiving data at a given transmission rate of W *bits/sec* from sender node i if (Grossglauser & Tse, 2001), (Gupta & Kumar, 2000)

$$SNIR = \frac{P_i(t)g_{ij}(t)}{N_0 + \frac{1}{L}\sum_{k \neq i} P_k(t)g_{kj}(t)} = \frac{P_i(t)g_{ij}(t)}{N_0 + \frac{1}{L}I} \geq \beta, \tag{1}$$

where the summation is over all sender nodes $k \neq i$, $P_i(t)$ is the transmitting power of sender node i, $g_{ij}(t)$ is the channel path gain from node i to node j, β is the *SNIR* level necessary for reliable communication, N_0 is the noise power spectral density, L is the processing gain of the system, and I is the total interference at node j. In order to facilitate the analysis, let us assume that no processing gain is used, i.e., $L = 1$, and that $P_i = P \; \forall i$. The channel path gain is considered to be a function of the distance, fading and path loss, so that

$$g_{ij}(t) = \frac{\chi_{ij}^2}{|X_i(t) - X_j(t)|^\alpha} = \frac{\chi_{ij}^2}{r_{ij}^\alpha}, \tag{2}$$

where χ_{ij}^2 is the Rayleigh fading from node i to node j, r_{ij} is the Euclidean distance between nodes i and j, and α is the path loss parameter.

The goal is to find an equation relating the total interference measured by a receiver node that is communicating with a neighbor node as a function of the number of total users n in the network. More precisely, we aim to obtain an expression for Eq. (1) as a function of n and calculate the limit of the SNIR and consequently the limiting spectral efficiency, as n goes to infinity.

3. Feasible Receivers Near a Sender

In order to obtain the interference generated by nodes outside the neighborhood of a receiver node, we first need to find the average radius size containing a sender node and how many feasible receivers are within this range.

If the density of nodes in the disk is

$$\rho = \frac{n}{total\;area} = \frac{n}{1} = n, \tag{3}$$

then the average radius for one sender node (r_0), for a uniform node distribution, is given by

$$1 = \theta\rho\pi r_0^2 = \theta n\pi r_0^2 \Rightarrow r_0 = \frac{1}{\sqrt{\theta n\pi}}. \tag{4}$$

Hence, the average number of receiving nodes, called $\overline{K}$, within r_0, assuming a uniform node distribution (Shepard, 1996), is

$$\bar{K} = nR\pi r_0^2 = (1-\theta)n\pi \left(\frac{1}{\sqrt{\theta n\pi}}\right)^2 = \frac{1}{\theta} - 1, \tag{5}$$

which is constant for a given θ. Eq. (5) is a benchmark for obtaining the average number of receiving nodes as a function of the network parameter θ.

Thus, the radius r_0 defines a cell (radius range) around a sender where $\bar{K}$ receiver nodes are nearby on average. The feasibility that all of those $\bar{K}$ nodes successfully receive the same data being transmitted by the sender is the subject of the next section.

4. Interference and Capacity Computation

In the previous section, the average radius r_0 containing one sender with $\bar{K}$ receiver nodes around on average was obtained. Suppose that one of the $\bar{K}$ receiving nodes is at the neighborhood[1] distance r_0. We want to show how the SNIR measured by this receiver behaves as the number of total nodes in the network (and therefore the number of total interferers) goes to infinity. We are interested in determing whether feasible communication between the sender and the farthest neighbor (with distance r_0) is still possible, even if the number of interferers grows.
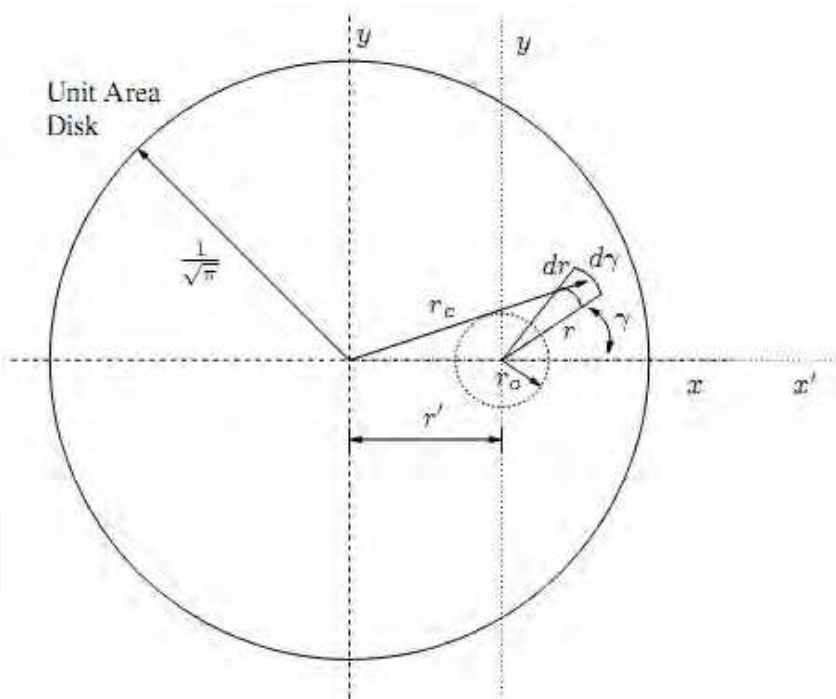

Fig. 1. Snapshot of the unit area disk at a given time t. At this time, the receiver node being analyzed is located at distance r' from the center while the sender is at distance r_0 from the receiver node.

---

[1] This represents the worst case scenario, because the other $\bar{K}-1$ neighbors are located either closer or at the same distance r_0 to the sender, so they measure either a stronger or the same SNIR value.

For a packet to be successfully received, Eq. (1) must be satisfied. Hence, consider a receiver at any location in the network for a given time t. Its distance from the center r' is shown in Figure 1, where $0 \leq r' \leq \frac{1}{\sqrt{\pi}} - r_0$.

Let us assume that the sender is at distance r_0 from this receiver and transmitting at constant power P, so that the power P_0 measured by this receiver is given by

$$P_0 = \frac{P\chi_0^2}{r_0^\alpha} , \tag{6}$$

where χ_0^2 is the Rayleigh fading from sender to receiver.

In order to obtain the overall expected interference at the receiver caused by all transmitting nodes in the disk, let us consider a differential element area $r\,dr\,d\gamma$ that is distant r units from the receiver and r_c units from the center of the network (see Figure 1). As consequence of the uniform mobility model, the steady-state distribution of the nodes is uniform (Bansal & Liu, 2003). Thus, the probability density function of the distance r_c to the center of the network is given by (Lau & Leung, 1992)

$$f_{R_c}(r_c) = \begin{cases} 2\pi r_c & \text{if } 0 \leq r_c \leq \frac{1}{\sqrt{\pi}} \\ 0 & \text{otherwise.} \end{cases} \tag{7}$$

Because the nodes are uniformly distributed in the disk, the transmitting nodes inside the differential element of area generate, at the receiver, the following amount of interference[2]

$$dI = \frac{P\chi^2}{r^\alpha}\theta\rho r\,dr\,d\gamma = \frac{P\chi^2}{r^{\alpha-1}}\theta n\,dr\,d\gamma . \tag{8}$$

The total interference is obtained by integrating Eq. (8) over the disk area and the result depends on the value of α. Accordingly, the following two cases are considered.

A. The case $\alpha > 2$

For some propagation environments (Rappaport, 2002) the path loss parameter is modeled to be always greater than two, i.e., $\alpha > 2$. In this case, the SNIR at the receiver located at distance r' from the center for a total of n nodes in the network is given in the following lemma.

Lemma 1. *At a given time t, for a receiver node located at distance r' from the center in a unit area disk network containing n mobile nodes uniformly distributed, where $\alpha > 2$, and assuming the sender located at distance r_0 from this receiver, then the receiver SNIR is given by*

---

[2] Because the nodes are uniformly distributed in the disk and n grows to infinity, we approximate the sum in Eq. (1) by an integral.

$$SNIR_{r'}(n) = \frac{Pe^{(\delta\sigma_s)^2}}{\dfrac{N_0}{(\theta n\pi)^{\frac{\alpha}{2}}} + \dfrac{2Pe^{(\delta\sigma_s)^2}}{\alpha - 2}q_{r',\alpha,\theta}(n)} \tag{9}$$

where $\delta = \frac{\ln(10)}{10}$, σ_s *is the standard deviation of the attenuation Gaussian random variable in decibels due to shadowing (Akl et al., 2001), and*

$$q_{r',\alpha,\theta}(n) = \left[1 - \frac{\int_0^\pi \left[\sqrt{\frac{1}{\pi} - (r'\sin\gamma)^2} - r'\cos\gamma \right]^{2-\alpha} d\gamma}{\pi^{\frac{\alpha}{2}}(\theta n)^{\frac{\alpha-2}{2}}} \right]^{-1}. \tag{10}$$

Proof of Lemma 1. By integrating Eq. (8) over the area of the disk, for $\alpha > 2$, we obtain the interference at the receiver located at a distance r' from the center for a total of n nodes in the network. Hence,

$$\begin{aligned}
E[I_{r'}(n)] = \int_{disk\,area} dI &= E\left[\int_0^{2\pi}\int_{r_0}^{r_m(r',\gamma)} \frac{P\chi^2}{r^{\alpha-1}}\theta n\, dr\, d\gamma \right] \\
&= Pe^{(\delta\sigma_s)^2}\theta n \int_0^{2\pi} \frac{r^{2-\alpha}}{2-\alpha} \Big|_{r_0}^{r_m(r',\gamma)} d\gamma \\
&= \frac{Pe^{(\delta\sigma_s)^2}\theta n}{\alpha-2} \int_0^{2\pi} \left\{ \frac{1}{r_0^{\alpha-2}} - \frac{1}{[r_m(r',\gamma)]^{\alpha-2}} \right\} d\gamma .
\end{aligned} \tag{11}$$

r_m is the maximum radius that r can have and is a function of the location r' and the angle γ (see Figure 1). To find this function, we can use the boundary disk curve (or circumference) equation expressed as a function of the x-axis and y-axis shown in Figure 1, i.e.,

$$x^2 + y^2 = \left(\frac{1}{\sqrt{\pi}} \right)^2. \tag{12}$$

Define $x = x' + r'$, $x' = r_m\cos\gamma$, and $y = r_m\sin\gamma$. Then, Eq. (12) becomes

$$(r_m\cos\gamma + r')^2 + (r_m\sin\gamma)^2 = \left(\frac{1}{\sqrt{\pi}} \right)^2 \Rightarrow r_m(r',\gamma) = \sqrt{\frac{1}{\pi} - (r'\sin\gamma)^2} - r'\cos\gamma . \tag{13}$$

By substituting this result in Eq. (11), we arrive at

$$E[I_{r'}(n)] = \frac{2Pe^{(\delta\sigma_s)^2}\theta n}{\alpha-2}\left[\frac{\pi}{r^{\alpha-1}} - f_\alpha(r') \right], \tag{14}$$

where

$$f_\alpha(r') = \int_0^\pi \frac{d\gamma}{\left[\sqrt{\frac{1}{\pi} - (r'\sin\gamma)^2} - r'\cos\gamma\right]^{\alpha-2}} \tag{15}$$

is a constant for a given position r'. For the case in which $\alpha = 4$, Eq. (15) reduces to

$$f_4(r') = \frac{\pi^2}{1 - 2\pi r'^2 + \pi^2 r'^4}. \tag{16}$$

The SNIR can be obtained by using Eqs. (1), (4), (6), and (14) to arrive at

$$
\begin{aligned}
SNIR_{r'}(n) &= \frac{E[P_0]}{N_0 + E[I_{r'}(n)]} = \frac{Pe^{(\delta\sigma_s)^2}}{\dfrac{N_0}{(\theta n\pi)^{\frac{\alpha}{2}}} + \dfrac{2Pe^{(\delta\sigma_s)^2}}{\alpha - 2} \cdot \dfrac{1}{1 - \dfrac{1}{\pi^{\frac{\alpha}{2}}(\theta n)^{\frac{\alpha-2}{2}}} \cdot f_\alpha(r')}} \\
&= \frac{Pe^{(\delta\sigma_s)^2}}{\dfrac{N_0}{(\theta n\pi)^{\frac{\alpha}{2}}} + \dfrac{2Pe^{(\delta\sigma_s)^2}}{\alpha - 2} \cdot q_{r',\alpha,\theta}(n)},
\end{aligned}
\tag{17}
$$

Where

$$q_{r',\alpha,\theta}(n) = \left[1 - \frac{1}{\pi^{\frac{\alpha}{2}}(\theta n)^{\frac{\alpha-2}{2}}} f_\alpha(r')\right]^{-1}, \tag{18}$$

which finishes the proof. ∎

From Eq. (9), taking the limit as $n \to \infty$, we obtain

$$
\begin{aligned}
SNIR &= \lim_{n\to\infty} \frac{Pe^{(\delta\sigma_s)^2}}{\dfrac{N_0}{(\theta n\pi)^{\frac{\alpha}{2}}} + \dfrac{2Pe^{(\delta\sigma_s)^2}}{\alpha - 2} \cdot q_{r',\alpha,\theta}(n)} \\
&= \begin{cases} \dfrac{\alpha - 2}{2} & \text{if } 0 \leq r' < \dfrac{1}{\sqrt{\pi}} - r_0 \\[2mm] \dfrac{\alpha - 2}{2} q_{r',\alpha,\theta}(n)(n \to \infty) & \text{if } r' = \dfrac{1}{\sqrt{\pi}} - r_0, \text{i.e.,} \\ & \text{the network boundary.} \end{cases}
\end{aligned}
\tag{19}
$$

From Eq. (10), $q_{r',\alpha,\theta}(n \to \infty) = q_{r',\alpha}(n \to \infty)$ because θ is a scale factor on n and it does not change the limit. Thus,

$$q_{r',\alpha,\theta}(n \to \infty) = \begin{cases} 1 & \text{if } 0 \leq r' < \frac{1}{\sqrt{\pi}} - r_0 \text{ and } \alpha > 2 \\ 1.47 & \text{if } r' = \frac{1}{\sqrt{\pi}} - r_0 \text{ and } \alpha = 3 \\ 1.33 & \text{if } r' = \frac{1}{\sqrt{\pi}} - r_0 \text{ and } \alpha = 4 \\ 1.27 & \text{if } r' = \frac{1}{\sqrt{\pi}} - r_0 \text{ and } \alpha = 5 \\ 1.23 & \text{if } r' = \frac{1}{\sqrt{\pi}} - r_0 \text{ and } \alpha = 6. \end{cases} \tag{20}$$

Therefore, from Eqs. (19) and (20), for $\alpha > 2$, the *SNIR* tends to a constant as $n \to \infty$.
From Lemma 1, the spectral efficiency (C) is straightly obtained and is given (in units of bits/s/Hz) by (Cover & Thomas, 1991)

$$C = \log_2[1 + SNIR_{r'}(n)] = \log_2\left[1 + \frac{Pe^{(\delta\sigma_s)^2}}{\frac{N_0}{(\theta n \pi)^{\frac{\alpha}{2}}} + \frac{2Pe^{(\delta\sigma_s)^2}}{\alpha - 2} \cdot q_{r',\alpha,\theta}(n)}\right]. \tag{21}$$

Accordingly, from Eqs. (9), (20) and (21), we conclude that the limiting spectral efficiency goes to a constant as $n \to \infty$ for $\alpha > 2$.

B. The case $\alpha = 2$

For the free space propagation environment (Rappaport, 2002), the path loss parameter is modeled to be equal to two, i.e., $\alpha = 2$. Thus, the total expected interference at the receiver located at distance r' from the center for a total of n nodes in the network is obtained by the following lemma, which proof is analogous to Lemma 1.

Lemma 2. *At a given time t, for a receiver node located at distance r from the center in a unit area disk network containing n mobile nodes uniformly distributed, where $\alpha = 2$, and assuming the sender located at distance r_o from this receiver, then the receiver SNIR is given by*

$$SNIR_{r'}(n) = \frac{Pe^{(\delta\sigma_s)^2}}{\frac{N_0}{\theta n \pi} + \frac{2Pe^{(\delta\sigma_s)^2}}{\pi} \cdot \int_0^\pi \ln\left[(\sqrt{\pi\theta n})\left(\sqrt{\frac{1}{\pi} - (r'\sin\gamma)^2} - r'\cos\gamma\right)\right] d\gamma}. \tag{22}$$

Consequently, the spectral efficiency is obtained (in units of bits/s/Hz) by (Cover & Thomas, 1991)

$$C = \log_2\left[1 + \frac{Pe^{(\delta\sigma_s)^2}}{\frac{N_0}{\theta n \pi} + \frac{2Pe^{(\delta\sigma_s)^2}}{\pi} \cdot \int_0^\pi \ln\left[(\sqrt{\pi\theta n})\left(\sqrt{\frac{1}{\pi} - (r'\sin\gamma)^2} - r'\cos\gamma\right)\right] d\gamma}\right]. \tag{23}$$

From Eq. (22), it is straightforward that $SNIR_{r'}(n) \to 0$ as $n \to \infty$. Therefore, the limiting spectral efficiency goes to zero as $n \to \infty$ for $\alpha = 2$.

5. Results

In this section, the analytical results elaborated in Section 4 are compared with Monte-Carlo simulations (Robert & Casella, 2004).

Figure 2 shows the spectral efficiency as function of n for $\alpha = 3$, $\theta = 1/3$ for distinct values of r'. Also, Figure 2 shows that the spectral efficiency remains constant when n goes to infinity and its does not depend on r' if $0 \le r' < \frac{1}{\sqrt{\pi}} - r_0$, and has the same value for any position of the receiver node, whether the position is at the center, close to the boundary, or at the middle region of the radius disk. Nevertheless, if the receiver node is at the boundary ($r' = \frac{1}{\sqrt{\pi}} - r_0$), then the limiting spectral efficiency is still a constant when n scales to infinity but it has a greater value.

Fig. 2. Spectral efficiency curves as a function of n for $\alpha = 3, \theta = 1/3$, $P = 1W, \sigma_s = 6$ and $N_0 = 5$ for the receiver node located at different positions in the network. In the legend, *model* is used for Eq. (21), while *simulation* is used for Monte-Carlo simulation.

Figure 3 illustrates the spectral efficiency behavior for different values of N_0 when $P = 1W$. As expected, the capacity diminishes when noise increases; however, the limiting capacity is the same regardless of noise because the interference effect dominates the denominator of Eq. (1) as $n \to \infty$.
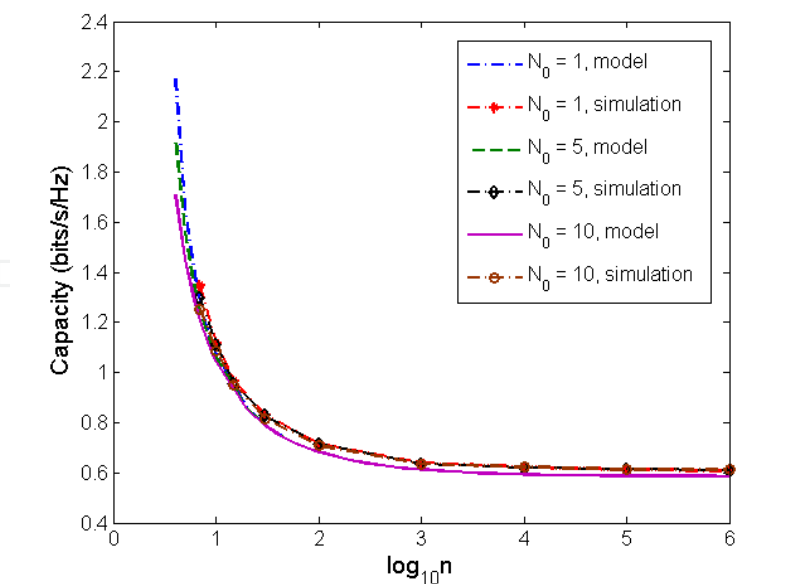
Fig. 3. Spectral efficiency curves as a function of n, for $\alpha = 3, \theta = 1/3, P = 1W$ and $\sigma_s = 6$, for different values of N_0. In the legend, *model* is used for Eq. (21), while *simulation* is used for Monte-Carlo simulation.

Figure 4 confirms that the limiting spectral efficiency does not depend on θ as observed in Section 4-A.
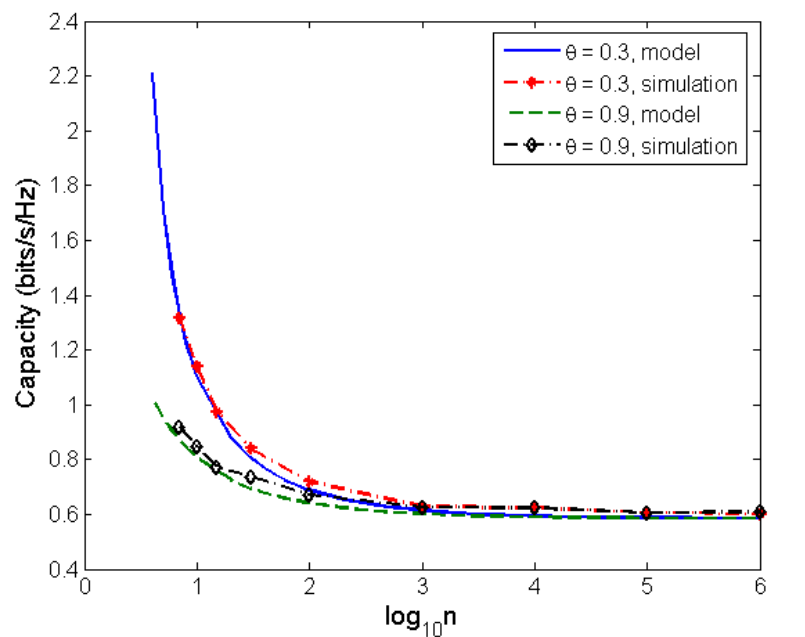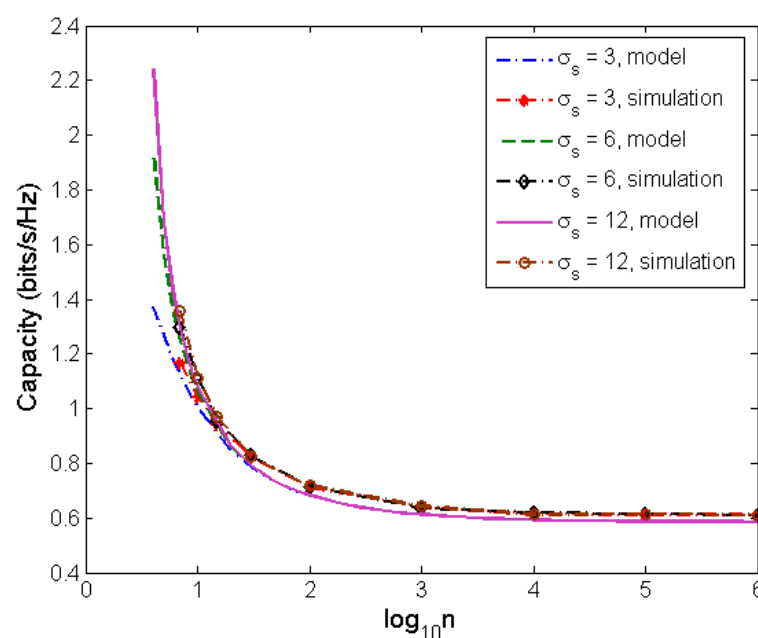

Fig. 4. Spectral efficiency curves as a function of n, for $\alpha = 3, N_0 = 5, P = 1W$ and $\sigma_s = 6$, for different values of θ. In the legend, *model* is used for Eq. (21), while *simulation* is used for Monte-Carlo simulation.

Figure 5 shows the spectral efficiency as function of n for different values of σ_s. It also illustrates that the capacity tends to a constant value as n scales to infinity regardless of σ_s.

Fig. 5. Spectral efficiency curves as a function of n, for $\alpha = 3, N_0 = 5, P = 1W$ and $\theta = 1/3$, for different values of σ_s. In the legend, *model* is used for Eq. (21), while *simulation* is used for Monte-Carlo simulation.
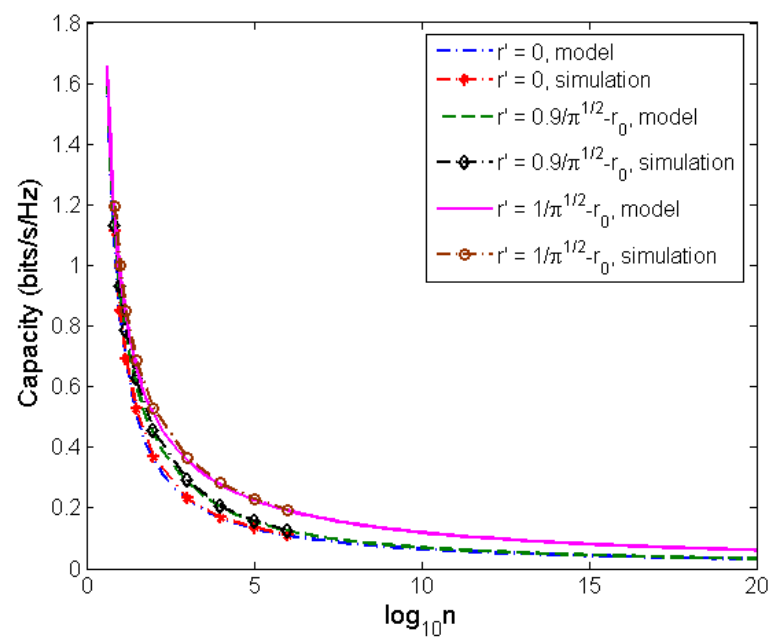

Fig. 6. Spectral efficiency curves as a function of n for $\alpha = 2, \theta = 1/3$, $P = 1W, \sigma_s = 6$ and $N_0 = 5$ for the receiver node located at different positions in the network. In the legend, *model* is used for Eq. (23), while *simulation* is used for Monte-Carlo simulation.

Figure 6 shows curves for spectral efficiency as function of n when $\alpha = 2$. Although the limiting capacity goes to zero as already observed in Section 4-B, the decay is not fast. We see that the spectral efficiency for a receiver node reaches 0.04 bits/s/Hz as the number of interferers approaches 10^{20}, i.e., the capacity falls very slowly, and it can allow feasible

communication between neighbor nodes for a finite number of users n. In addition, the capacity is about 0.066 bits/s/Hz for a receiver at the boundary of the network for this same number of interferers. Note that we have plotted points up to $n = 10^{20}$ for the model, while the simulations were plotted up to $n = 10^6$ due to computer limitation.

6. A Technique to Attain a Desired Value for The θ Parameter

Another challenge associated with this study is how a node can efficiently set its state (sender or receiver) in order to the network attain a given θ. The work presented by Grossglauser and Tse (Grossglauser & Tse, 2001), and supplemented by Moraes (Moraes et al., 2007) shows analytically and by simulation that the maximum throughput for a wireless ad hoc network is achieved when the fraction of sender nodes (θ) is approximately $\frac{1}{3}$ of the total nodes in the network. However, to the best of our knowledge, there are no studies in the literature on MAC protocols that seek this distribution autonomously and in a distributed way.

The technique suggested here consists of a simplified part of a MAC layer protocol. Similar to the Traffic Adative Medium Access (TRAMA) protocol (Rajendran et al., 2003), our scheme has the requirement to be synchronized with cyclical periods of contention followed by transmission in which some nodes are capable of taking control of close neighbors, as found in IEEE 802.15.4 - ZigBee (ZigBee Alliance, 2009). This technique, restricted only to the contention period, is intended to be autonomous and able to distribute the states of the nodes according to the θ parameter.

Considering the node distribution as described in Section 2 and that each node has its unique identification (ID), the node with the lowest ID controls the network and it is called the coordinator node of the network.

The communication among nodes follows cycles which are divided in contention and transmission phases. The contention period is divided in following three phases, respectively. The announcement is the period in which each node sends its packet identification number. The dissemination is the phase when the coordinator node sends its identification to all nodes of the domain. Finally, there is the distribution phase where the node coordinator sends a random sequence indicating the status (sender or receiver) that each node in the network must assume during the following transmission period according to the θ parameter previously scheduled.

Figure 7 presents the results of a simulation implemented in JAVA (Java, 2009), using the shuffle method of Class Collections (JavaClassCollections, 2009) for the random distribution of the states (sender and receiver), which are displayed as fraction of times that three nodes randomly chosen, over 100 cycles, were senders. It is observed that the three randomly chosen nodes tend to converge their sender fraction of times to $\theta = \frac{1}{3}$ as expected.
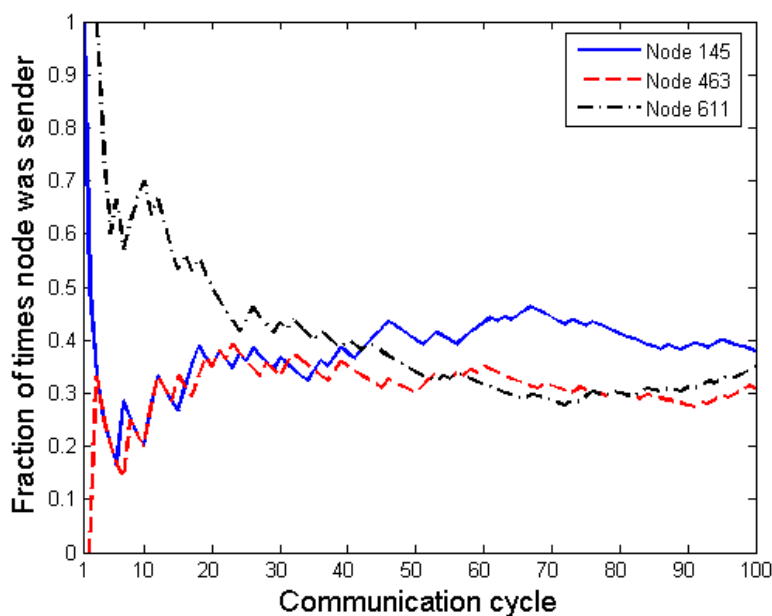
Fig. 7. Evolution of the fraction of times that three randomly chosen nodes were sender over the simulated cycles for $\theta = 1/3$ and $n = 1000$.

The technique suggested here does not consider other medium access issues like channel admission control, collision resolution, node failure, etc., which is subject of future work.

7. Conclusions

We have analyzed interference effects and spectral Shannon capacity (or spectral efficiency) for mobile ad hoc networks using a communication channel model, which considers Euclidean distance, path loss, fading and a random mobility model. We found that, for a receiver node communicating with a close neighbor where the path loss parameter α is greater than two, the resultant signal to noise and interference ratio (SNIR) and consequently the spectral efficiency tend to a constant as the number of nodes n goes to infinity, regardless of the position of the receiver node in the network. Therefore, for the studied model, communication is feasible for near neighbors when the number of interferers scales. Furthermore, for the receiver nodes located at the boundary of the circular network, we show that they suffer less interference than those located inside attaining higher capacity. Also, for the case where α is equal to two, the capacity was shown to go to zero as n increases; however, the decay is very slowly making local communication still possible for a finite n. Model and Monte-Carlo simulation results present good agreement and validate the interference and Shannon capacity investigation performed.

It was also proposed a technique for autonomous and distributed allocation of states (sender or receiver) of nodes based on the parameter θ. Future work can consider MAC layer issues like admission control and collisions, as well as power control and other types of mobility which results in other distributions of nodes in the network, and how they affect the capacity.

Acknowledgements

8. References

Akl, R., Hedge, M., Naraghi-Pour, M., & Min, P. (2001). Multicell CDMA Network Design, *IEEE Transactions on Vehicular Technoogy*, vol. 50, no. 3, pp. 711-722.

Bansal, N. & Liu, Z. (2003). Capacity, delay and mobility in wireless ad-hoc networks, *Proc. of IEEE Infocom*, San Francisco, CA.

Cover, T. M. & Thomas, J. A. (1991), In: *Elements of Information Theory*. John Wiley & Sons.

Deng, J., Han, Y. S., Chen, P. N. & Varshney, P. K. (2004). Optimum transmission range for wireless ad hoc networks, *Proc. of IEEE WCNC*, Atlanta, GA.

Gobriel, S., Melhem, R. & Mossé, D. (2004). A unified interference/collisionanalysis for power-aware ad hoc networks, *Proc. of IEEE Infocom*, Hong Kong.

Grossglauser, M. & Tse, D. (2001). Mobility increases the capacity of wireless ad-hoc networks, *Proc. of IEEE Infocom*, Anchorage, AK.

Gupta, P. & Kumar, P. R. (2000). The capacity of wireless networks, *IEEE Transactions on Information Theory*, vol. 46, no. 2, pp. 388–404.

Hajek, B.; Krishna, A. & LaMaire, R. O. (1997). On the capture probability for a large number of stations, *IEEE Transactions on Communications*, vol. 45, no. 2, pp. 254–260.

Java Class Collections (2009). On http://java.sun.com/j2se/1.3/docs/api/java/util/Collections.html

Java Language (2009). On http://java.sun.com

Knopp, R. & Humblet, P. A. (1995). Information capacity and power control in single-cell multiuser communications, *Proc. of IEEE ICC*, Seattle, WA.

Lau, C. T. & Leung, C. (1992). Capture models for mobile packet radio networks, *IEEE Transactions on Communications*, vol. 40, no. 5, pp. 917–925.

Liu, X. & Haenggi, M. (2005). Performance analysis of rayleigh fading ad hoc networks with regular topology, In *Proc. of IEEE Globecom*, St. Louis, MO.

Moraes, R. M. de, Buarque, C. E. & Araujo, F. P. (2008). Shannon Capacity for a Simple Communication Channel Model in Dense MANETs, *Proc. Of IEEE IWCMC*, Crete, Greece.

Moraes, R. M. de, Sadjadpour, H. & Garcia-Luna-Aceves, J. J. (2007). Taking full advantage of multiuser diversity in mobile ad hoc networks. *IEEE Transactions on Communications*, vol. 55, pp. 1202-1211.

Qin-yun, D.; Xiu-lin, H.; Hong-yi, Y. & Jun, Z. (2005). On the capacity of wireless ad-hoc network basing on graph theory, In: *Lecture Notes in Computer Science*, vol. 3421/2005, pp. 353–360.

Rajendran, V. ; Obraczka, K. & Garcia-Luna-Aceves, J. J. (2003). Energy-Efficient, Collision-Free Medium Access Control for Wireless Sensor Networks, *Proceedings of ACM SenSys 03*, Los Angeles, CA.

Rappaport, T. S. (2002). In: *Wireless Communications: Principles and Practice*. Prentice Hall.

Rickenbach, P. von ; Schmid, S. ; Wattenrofer, R. & Zollinger, A. (2005). A robust interference model for wireless ad-hoc networks, *Proc. of IEEE WMAN*, Denver, CO.

Robert, C. P. & Casella, G. (2004). In: *Monte Carlo Statistical Methods*. Springer-Verlag.

Shepard, T. J. (1996). A channel access scheme for large dense packet radio networks, *Proc. of ACM SigComm*, San Francisco, CA.

Tobagi, F. & Kleinrock, L. (1975). Packet switching in radio channels: Part ii - the hidden terminal problem in carrier sense multiple-access and the busy-tone solution, *IEEE Transactions on Communications,* vol. COM-23, no. 12, pp. 1417–1433.

ZigBee Alliance (2009). IEEE 802.15.4, ZigBee standard. On http://www.zigbee.org

Trends in Telecommunications Technologies

Edited by Christos J Bouras

The main focus of the book is the advances in telecommunications modeling, policy, and technology. In particular, several chapters of the book deal with low-level network layers and present issues in optical communication technology and optical networks, including the deployment of optical hardware devices and the design of optical network architecture. Wireless networking is also covered, with a focus on WiFi and WiMAX technologies. The book also contains chapters that deal with transport issues, and namely protocols and policies for efficient and guaranteed transmission characteristics while transferring demanding data applications such as video. Finally, the book includes chapters that focus on the delivery of applications through common telecommunication channels such as the earth atmosphere. This book is useful for researchers working in the telecommunications field, in order to read a compact gathering of some of the latest efforts in related areas. It is also useful for educators that wish to get an up-to-date glimpse of telecommunications research and present it in an easily understandable and concise way. It is finally suitable for the engineers and other interested people that would benefit from an overview of ideas, experiments, algorithms and techniques that are presented throughout the book.

INTECH

open science | open minds